ASME Journal of Micro- and Nano-Manufacturing. **4** (2) 021005 (2016).
dx.doi.org/10.1115/1.4032891

Vacuum venting enhances the replication of nano/micro-features in microinjection molding process

Seong Ying, Choi, first author[1]
School of Mechanical & Materials Engineering, University College Dublin, Ireland
e-mail: seong.choi@ucd.ie

Nan, Zhang, second author
School of Mechanical & Materials Engineering, University College Dublin, Ireland
e-mail: nan.zhang@ucd.ie

J. P. Toner, third author
School of Mechanical & Materials Engineering, University College Dublin, Ireland
e-mail: jp.toner@ucdconnect.ie

G. Dunne, fourth author
School of Mechanical & Materials Engineering, University College Dublin, Ireland
e-mail: garreth.dunne@ucdconnect.ie

Michael D. Gilchrist, corresponding author
School of Mechanical & Materials Engineering, University College Dublin, Ireland
e-mail: michael.gilchrist@ucd.ie
Member, ASME

[1] Corresponding author: Professor of Mechanical Engineering and Head of School.

ABSTRACT

Vacuum venting is a method proposed to improve feature replication in microparts that are fabricated using micro injection molding (MIM). A qualitative and quantitative study has been carried out to investigate the effect of vacuum venting on nano/micro feature replication in MIM. Anodized aluminium oxide containing nanofeatures and a bulk metallic glass tool mold containing micro features were used as mold inserts. The effect of vacuum pressure at constant vacuum time, and of vacuum time at constant vacuum pressure on the replication of these features is investigated. It is found that vacuum venting qualitatively enhances the nano-scale feature definition as well as increases the area of feature replication. In the quantitative study, higher aspect ratio features can be replicated more effectively using vacuum venting. Increasing both vacuum pressure and vacuum time are found to improve the depth of replication, with the vacuum pressure having more influence. Feature orientation and final sample shape could affect the absolute depth of replication of a particular feature within the sample.

1 INTRODUCTION

Micro injection molding (MIM) is a polymer processing method which is by far the most common method in manufacturing polymer microparts in large quantities. MIM has become more popular due to the growing market for microelectromechanical systems (MEMS) and microsystems (MST) [1,2]. Compared to conventional injection molding, MIM is capable of more precise microfeature replication due to its having a more precise electrical control system compared to the hydraulic system of conventional injection molding. However, due to the miniaturised features and thinner mold cavity, the micro injection molding process has major challenges including significantly higher shear rates during filling, and more difficult filling due to faster heat loss resulting in premature solidification of polymer melt [1-3].

Numerous studies have been carried out to study nano/micro feature replication in polymer microparts during the micro injection molding process [4-6]. Several methods have been proposed as methods to improve nano/micro feature replication, such as using variotherm (or rapid thermal cycling) and vacuum venting method [1-3,7].

Vacuum venting has been used as a way to improve feature replication in both conventional and micro injection molding [1-3]. Inadequate venting in conventional injection molding has caused some common defects such as short-shot, poor appearance, burn marks and even permanent mold damage, and it is believed that the defects could be accentuated in MIM since the process involves high injection velocity and pressure, and rapid cooling [1-3,8]. The interactions between vacuum venting and (1) feature size, (2) material type, i.e. rheological properties, and (3) processing parameters such as injection velocity, pressure and mold temperature has been studied. The efficiency of vacuum venting in feature replication often can be quantified in terms of depth ratio (DR), i.e. ratio of the feature height in the molded part to the feature height in the tooling, which can also be expressed in percentage terms [6,8].

Yoon et al. [8] summarized a list of studies on the effect of vacuum venting for micro injection molding. Most studies used positive mold features, with the feature size being mainly in tens of microns in size and not smaller than 5micron or at the sub-micron scale.

In this study, we have carried out separate qualitative and quantitative analyses to investigate the efficiency of vacuum venting on the replication of negative mold features sized smaller than 5 micron and also at the sub-micron scale. Anodized

aluminium oxide (AAO) film, a nanostructured material containing cylindrical-hexagonal pores aligned perpendicular to the surface and made with electrochemically oxidized aluminium, was used as a mold template in our qualitative analysis. In our quantitative study, negative features, specifically trenches that were smaller than 5 microns and were aligned in three different directions (parallel and perpendicular to the melt flow direction and at 45° to the melt flow direction), were fabricated using focused ion beam milling (FIB) onto bulk metallic glass (BMG) as a mold template. The effect of vacuum pressure at constant vacuum time, and the effect of vacuum time at constant vacuum pressure on feature depth replication, is investigated in both studies. The effect of aspect ratio and feature alignment on the replication depth of the features was also analysed in our quantitative analysis.

2 EXPERIMENTAL

2.1 Materials and Processing

Vacuum venting studies were carried out using a Fanuc Roboshot S-2000i 15B reciprocating micro injection molding machine that was connected to a vacuum pump (piCLASSIC xi x1, Piab) which had a gas supply from a compressor. Vacuum suction was introduced shortly before the mold closed until the end of the packing phase within the injection cycle. A cassette mold with interchangeable mold inserts was used, as shown in Fig. 1(a), while the vacuum set up was shown in Fig. 1(b) and (c).

Two polymer materials, cyclic olefin copolymer (COC), (Topas 8007X10, Topas Advanced Polymers, melt flow index 32.64 g/min, ISO 1133, 260°C/2.16kg) and

poly(methyl methacrylate) (PMMA), (Altuglas VS-UVT, melt flow index 24g/10min, 230°C/10min) were used in the quantitative and qualitative studies, respectively. The polymer processing conditions (listed in Table 1) are chosen based on ease of demoulding without damaging either the AAO template or the BMG mold during a quick trial. They are not optimized and merely serve as constants, since the main focus of the present paper is vacuum time and vacuum pressure. The final polymer samples that were manufactured were square shaped with rounded corners in the dimension of 26mm x 26mm x 1.1mm thick (see Figure 1(d)).

2.2 Qualitative measurement: AAO template

A cassette mold with mold inserts, which contained inter-changeable mold strips were used. AAO film (6563-6565, Synkera Technologies Inc.) with a nominal pore diameter of 55nm was wrapped around a polished stainless steel mold strip and inserted into the mold insert (see arrow in Fig.1(a)). The AAO mold template was examined using SEM prior to MIM, shown in Fig. 2(a). COC was used to replicate the nanofeatures on the AAO mold template. Vacuum suction was introduced at different negative gauge pressures (approximately -33.25 kPa and -65 kPa) and for different time durations (3 and 10 seconds), mainly after the mold closed until the end of packing phase within the injection cycle. The nanofeatures on COC samples were then gold-coated and examined under scanning electron microscope (SEM, FEI QuantaTM) under a magnification of 50,000x.

2.3 Quantitative measurement: Focus-ion-beam processed BMG template

Three microfeatures were fabricated as negative trenches aligned in three different directions relative to the flow direction (horizontal, vertical and at 45°) with a range of different aspect ratios (depth-to-width ratio). These were machined onto a BMG mold strip using the FIB milling process, as shown in Fig. 3. The depths of the trenches were measured using an optical profilometer, and three width measurements along the trenches were taken using image analysis software (ImageJ). The aspect ratios (A.R.), i.e. depth-to-width values calculated using the average values, are listed in Table 2. The BMG mold strip containing the features was inserted into the same cassette mold at the same location as the AAO mold template (see arrow in Fig. 1(a)). PMMA was used as the material for feature replication. Vacuum suction was introduced at different negative gauge pressures (0, -25, -45 and -65 kPa) at a constant vacuum time (2s), and a constant vacuum gauge pressure of approximately -35kPa for different times (0, 1.0, 2.0 and 6.0 seconds). The 3D dimensions of the replicated features (n=3) appearing as ridges were measured using an optical profilometer (Wyko NT1100) at a magnification of 50x.

3 RESULTS AND DISCUSSIONS

3.1 Qualitative Analysis

Fig. 2(b)-(f) show the results of our qualitative analysis, presenting the replication of AAO template without (Fig. 2(b)) and with vacuum venting (Fig. 2(c)-(f)). COC samples injection molded under ordinary conditions, i.e. no vacuum applied, were used as a control in the study (Fig. 2(b)). It can be seen that without the application of vacuum suction, only very shallow ‘dimples’ were formed. In Fig. 2(c) and 2(d), both were injection

molded under different vacuum gauge pressures but for the same vacuum time. Under weaker vacuum gauge pressure at a vacuum time of 3s (Fig. 2(c)), deeper 'dimples' were formed, but limited 'hexagonal' structures were replicated, which was the shape of the AAO nano-sized pore. This indicated that there was still air trapped within the AAO pore, resulting in polymer melt solidification before filling of the AAO pore, forming these deeper 'dimples'. When the applied negative gauge pressure was doubled, it resulted in a mixture of 'dimples'/holes and hexagonal structures, see Fig. 2(d). When increasing the vacuum time, more distinctive hexagonal features were observed at both pressures (Fig. 2(e) and 2(f)), with the higher vacuum gauge pressure resulting in successful formation of hexagonal structures over a larger area. Due to the small size of the feature (~55nm), it was difficult to quantify the depth of feature using techniques such as SEM or an optical profilometer. Atomic force microscope (AFM) was used in a recent study to characterize a feature in the range of 500 nm [9], but that feature is 9-10 times larger than the feature used in this study. Thus, a quantitative study was carried out using FIB milled micro structures on BMG mold.

3.2 Quantitative Analysis

For quantitative analysis, three Z-shape features were FIB milled onto the BMG mold, see Fig. 3. The Z-channels are all of the same depth, but the width varies into a range of ratio aspects. Only the middle part of the Z-channels was used to study the effect of vacuum venting, where the spacing is the same. This is to simulate the necessity of aligning the channels in a microfluidic part that act as a fluid transporter, therefore additional trenches were added forming a 'Z' shape instead of a rectangular trench.

3.2.1 Vacuum Gauge Pressure as Variable

Fig. 4 shows the depth replication at increasing maximum vacuum gauge pressures applied in different trenches (channel 1-7) at a constant 2s vacuum time. The results show that the filling increases with the increase of applied vacuum pressure. The depth replication seemed to reach its maximum at around ~-45kPa vacuum gauge pressure in most channels, with an overall improvement of depth replication ranges between 1.33~7.52%, reaching a plateau value once the vacuum gauge pressure exceeded ~-45kPa. While at -65kPa vacuum gauge pressure, the overall improvement of depth replication ranges between 0.65~7.09%. The ranges seemed to be much wider than that reported in the literature (4.6~5.4% and 2.7~4.1%) [8,10], which is probably due to the wide range of aspect ratios used and the fact that air entrapment is more significant for small features. A 1-sample t-test was carried out to compare the depth replication under control conditions to each vacuum gauge pressure that had been applied. This indicated that 5 or more channels out of 7 gave a significant difference ($p<0.05$) at both vacuum gauge pressures of ~-45 and ~-65 kPa, with slight variation in channels within the same feature.

3.2.2 Vacuum time as variable

To investigate the effect of vacuum time at constant vacuum pressure, different vacuum times were applied starting from when the mold closed. The result is shown in Fig. 5.

Depth replication generally improves as the applied vacuum time is increased, reaching a maximum at 2s and a plateau at 6s. Similar to the study with vacuum pressure

as the variable, the depth replication increases with the decrease in feature aspect ratio, with the exception of channel 7. Since channel 7 showed lower depth replication regardless of whether vacuum pressure or vacuum time applied, this can be explained by the formation process of the polymer features. Depending on the material, temperature and feature dimensions, the polymer melt filling into the micro cavity experiences fast solidification upon heat conduction and convention from the wall of the micro cavity and the flow front. When increasing the feature width, with the exception of the fast solidification skin layer, large features may have liquid polymer in their core and solidification of such liquid polymer causes a relatively large amount of volume shrinkage, which reduces the depth replication of the feature. In addition, because of viscoelasticity, polymer melts and solids retract more if the width of a feature is larger [11].

The maximum vacuum time that can be applied is 6s, in which the vacuum was applied throughout the injection cycle until the end of the packing stage. Similar to vacuum pressure, it is found that the vacuum time which gives the best depth replication is 2s, with the improvement of depth replication ranges between 0.88~5.94%, compared to 1.40~4.90% at a vacuum time of 6s. Even though the minimum improvement in depth replication of 6s vacuum time is higher than that in 2s, most of the channels showed a higher improvement in the depth replication for the vacuum time of 2s. A 1-sample t-test comparing the results of various vacuum times was applied to the results of the control conditions; this showed that depth replication in 4 or more channels out of the 7 channels within each feature showed a significant difference ($p<0.05$) at a vacuum time of 2s.

No vacuum time of between 2~6s was considered as the experiment had been designed so that the vacuum would only be applied at the early stage of the injection phase, while the injection time is estimated to be less than 1s (0.12s). The reduction in depth replication at a vacuum time of 6s could be due to cooling of the mold surface via the removal of hot air, and solidification of polymer melt due to the longer application of vacuum time [8]. The results also suggest that the feature forming process is continuous throughout the packing stage.

3.2.3 Aspect ratio and feature orientation

Channels with aspect ratios ranging from 0.72 to 9.86 were used in this study. Channel 7 in all three features has the lowest aspect ratio but it only achieved a depth of replication that was comparable to that of channel 3. Although it has been reported that non-crystalline PMMA allows better replication than crystalline polymers such as PP and HDPE, with depth replication being achieved in high aspect ratios, i.e. as high as 12, without the use of vacuum [12]. However, the feature width size used in [12] was significantly larger than that of this study (20, 10 and 2μm), and the mould temperature that had been used was also much higher (90~150°C). Another study also reported that the increase of width and depth improves the melt flow, but the melt fill of micro features does not increase linearly with the increase of the sizes [13]. The lower filling/ depth replication in channel 7 could be due to melt retraction of this particular polymer at this particular temperature and possible volumetric shrinkage, as discussed in Section 3.2.2.

The effect of feature orientation on depth replication under different vacuum gauge pressures and vacuum times was also investigated in this study. This is important

because the channels should have the flexibility to form towards different directions in order to transport the microfluidic content to different parts of the microfluidic device and fully utilize each compartment within the device. Fig. 6 shows a scatter plot of depth replication (%) in each oriented feature as a function of aspect ratios. A general trend was observed, namely that the horizontal channels achieve higher depth replication, followed by 45° features with the vertical channels having the least depth replication. If the flow direction of the melt front plays a role in filling of these features, the filling percentage would vary either in the sequence of vertical > horizontal > diagonal or vertical < horizontal < diagonal. Since the sequence observed was horizontal > diagonal > vertical, this suggests that the location of the features on the mold did not affect the replication outcome. The lowest depth replication achieved in the vertical channels was probably due to the feature's higher aspect ratio (see Table 2). This coincides with studies suggested that better replication can be achieved with features having lower aspect ratios [11,12]. However, features aligned at 45° and which had lowest aspect ratios showed lower depth replication compared to the horizontal features. A study showed that vertical channels parallel to the melt flow direction in a dog-bone sample gave higher filling compared to horizontal channels which are perpendicular to the melt direction [6]. The better filling in the horizontal channels in this present study indicated that sample shape could affect the filling of features with a particular orientation [11].

The feature orientation also varies the depth replication at different vacuum gauge pressure. In vertical channels, the highest vacuum pressure of ~-65 kPa gave either equivalent or lower depth replication. But in the 45° and the horizontal channels, ~-65kPa

vacuum gauge pressure generally gave a better depth replication compared to that of ~-45kPa. This might be due to the current venting system – the air in the mould cavity is extracted via gaps between 4 pins (appear as 4 holes in each corner of the sample in Figure 1) and gaps between mould insert and mould plate. As the mould insert is rectangular shape, air within the mould cavity probably has higher tendency to be evacuated at shortest distance (or flow path length) from the centre, which is via the gaps between the pins (45° to the features) or the lateral dimension of the rectangular mould insert (horizontal to the features). In terms of vacuum time, 45° features also yielded a similar improvement in depth replication for vacuum times of 2s and 6s, suggesting the local air pressure in the 45° channels was more even than in the features that were aligned in the other two orientations. This more even local air pressure is probably contributed by the shortest distance of the 4 pins from the features.

4 CONCLUSION

Both qualitative and quantitative analyses of vacuum applied during the injection phase in the micro injection molding process has shown the improvement of the feature replication, either by creating clearly, more defined features over larger areas (qualitative) or in terms of actual depth (quantitative).

It is found that, regardless of whether vacuum is applied, both feature size (channel width) and feature orientation play significant roles in feature replication. The reduction of depth replication in channel 7 may indicate that it is best not to include features with large differences in A.R. when designing a final product, which may lead to

lower depth replication. However it might be possible to resolve this issue with more rigorous process optimisation for a particular polymer material.

In the quantitative analysis, the depth replication can be improved by 1.33~7.52% by varying the vacuum pressure, and 0.88~5.94% by varying the vacuum time. This indicates that vacuum pressure plays a more significant role than vacuum time in improving the depth replication. The application of vacuum pressure in this study allows for better depth replication in features of higher aspect ratio. It is also found that a particular sample shape may vary the depth of replication in features of a particular orientation. Certain feature orientation may give a more even filling by having a more evenly distributed air pressure, depending on the venting system set up to extract air in a particular way.

Future work following on from this study include investigating the filling of negative features with different spacings in between the features, increasing data collection for vacuum times between 2~6s at constant vacuum gauge pressure. The vacuum system can be improved by adding extra sensors such as air transducer [14], for online monitoring and data collection. Evaluating the effect of vacuum venting time and pressure with the main influential process parameters should also be included as potential future work.

ACKNOWLEDGMENT

The authors acknowledge financial support from Enterprise Ireland (Grant No. CFTD/2012/2022) and the European Regional Development Fund, and the assistance of Mr. J. Gahan, Mr. R. Byrne and Mr. Q. Su in vacuum venting setup and mould strip fittings.

FUNDING

Enterprise Ireland (EI) (Grant No. CFTD/2012/2022)

European Regional Development Fund

REFERENCES

[1] Giboz, J., Copponnex, T., and Mélé, P., 2007, "Microinjection molding of thermoplastic polymers: a review," J. Micromech. Microeng., **17**(6), pp. R96-R109. DOI: 10.1088/0960-1317/17/6/R02

[2] Yang, C., Yin, X., and Cheng, G., 2013, "Microinjection molding of microsystem components: new aspects in improving performance," J. Micromech. Microeng., **23**(9), pp. 093011. DOI:10.1088/0960-1317/23/9/093001

[3] Zhiltsova. T. V., Oliveira, M. S. A., and Ferreira, J. A., 2013, "Integral approach for production of thermoplastics microparts by injection molding," J. Mater. Sci., **48**(1), pp. 81-94. DOI: 10.1007/s10853-012-6669-7

[4] Zhang, N., and Gilchrist, M. D., 2012, "Characterization of thermo-rheological behavior of polymer melts during the micro injection moulding process," Polym. Test., 2012; **31**(6), pp.748-758. DOI: 10.1016/j.polymertesting.2012.04.012

[5] Zhang, N., Choi, S. Y., and Gilchrist, M. D., 2014, "Flow induced crystallization of poly(ether-block-amide) from the microinjection molding process and its effect on mechanical properties," Macromol. Mater. Eng., **299**(11), pp. 1362-1383. DOI:10.1002/mame.201300459

[6] Zhang, N., Chu, J. S., Byrne, C. J., Browne, D. J., and Gilchrist, M. D., 2012, "Replication of micro/nano-scale features by micro injection molding with a bulk metallic glass mold insert," J. Micromech. Microeng., **22**(6), pp. 065019. DOI: 10.1088/0960-1317/22/6/065019

[7] Zhang, N., Byrne, C. J., Browne, D. J., and Gilchrist, M. D., 2012, "Towards nano-injectionmolding," Mater. Today, **15**(5), pp. 216-221. DOI: 10.1016/S1369-7021(12)70092-5

[8] Yoon, S. H., Padmanabha, P., Cha, N. G., Mead, J. L., and Barry, C. M. F., 2011, "Evaluation of vacuum venting for micro-injection molding," Int. Polym. Process. XXVI, **26**(4), pp. 346-353. DOI: 10.3139/217.2308

[9] Menotti, S., Hansen, H. N., Bissacco, G., Calaon, M., Tang, P. T., Ravn, C., "Injection molding of nanopatterned surfaces in the sub-micrometer range with induction heating aid," Int. J. Adv. Manuf. Technol., **74**(5), pp. 907-916. DOI: 10.1007/s00170-014-6010-5

[10] Ong, N. S., Zhang, H., Woo, and W. H., 2006, "Plastic injection molding of high-aspect ratio micro-rods," Mater. Manuf. Process., **21**(8), pp. 824-831. DOI: 10.1080/03602550600728083

[11] Berger, G. R., Gruber, D. P., Friesenbichler, W., Teichert, C., and Burgsteiner, M., 2011, "Replication of Stochastic and Geometric Micro Structures – Aspects of Visual Appearance," Int. Polym. Process. CCVI, **26**(3), pp. 313-322. DOI: 10.3139/217.2451

[12] Liou, A. C., and Chen, R. H., 2006, "Injection molding of polymer micro- and sub-micron structures with high-aspect ratios," Int J Adv Manuf Technol, **28**(11-12), pp. 1097-1103. DOI 10.1007/s00170-004-2455-2

[13] Sha, B., Dimov, S., Griffiths, C., Packianather, M. S., 2007, "Micro-injection moulding: Factors affecting the achievable aspect ratios," Int J Adv Manuf Technol, **33**(1-2), pp. 147-156. DOI 10.1007/s00170-006-0579-2

[14] Griffiths, C. A., Dimov, S. S., Scholz, S., Tosello, G., “Cavity Air Flow Behavior During Filling in Microinjection Molding,” J. Manuf. Sci. Eng., **133**(1), pp. 011006-1-011006-10. DOI: 10.1115/1.4003339

Figure Captions List

Fig. 1 (a) Cassette mold showing AAO mold template (arrow, left) and BMG mold strips (right); (b) cassette mold connected to vacuum pump; (c) illustration of mold cross-section; (d) sample shape (front view) and feature location for quantitative analysis.

Fig. 2 SEM images of (a) AAO template, (b) COC samples under no vacuum, (c) COC sample under ~-33.25 kPa for 3 seconds, (d) COC sample under ~-65 kPa for 3 seconds, (e) COC sample under ~-33.25 kPa for 10 seconds; and (f) COC sample under ~-65 kPa for 10 seconds (scale bar: 1μm).

Fig. 3 SEM image of FIB features on BMG: (a) position of features (scale bar:300μm), (b) horizontal channels (scale bar: 50μm), (c) vertical channels (scale bar: 40μm), and (d) 45° channels (scale bar: 50μm). Red arrow represents direction of gate from the microfeatures.

Fig. 4 Depth replication (%) as a function of maximum vacuum gauge pressure applied for (a) horizontal channels, (b) vertical channels, (c) 45° channels, at constant vacuum time 2s for channels 1-7 (n=3).

Fig. 5 Depth replication (%) as a function of vacuum time applied for (a) horizontal channels, (b) vertical channels, (c) 45° channels, at constant vacuum gauge pressure of ~45kPa for channels 1-7 (n=3).

Fig. 6 Effect of different channel directions on depth of replication at (a) control condition (no vacuum applied), (b) maximum vacuum gauge pressure of

~-45 kPa at 2s vacuum time; (c) maximum vacuum gauge pressure ~-65kPa at 2s vacuum time; and (d) vacuum gauge pressure of vacuum time of ~-45 kPa at 2s vacuum time. Note: comparison of (b) and (c) for different vacuum gauge pressure and comparison of (b) and (d) for different vacuum time.

Table Caption List

Table 1 Processing conditions for polymer samples.

Table 2 Calculated depth-to-width/ aspect ratio (A.R.) of the trenches in each channel direction.

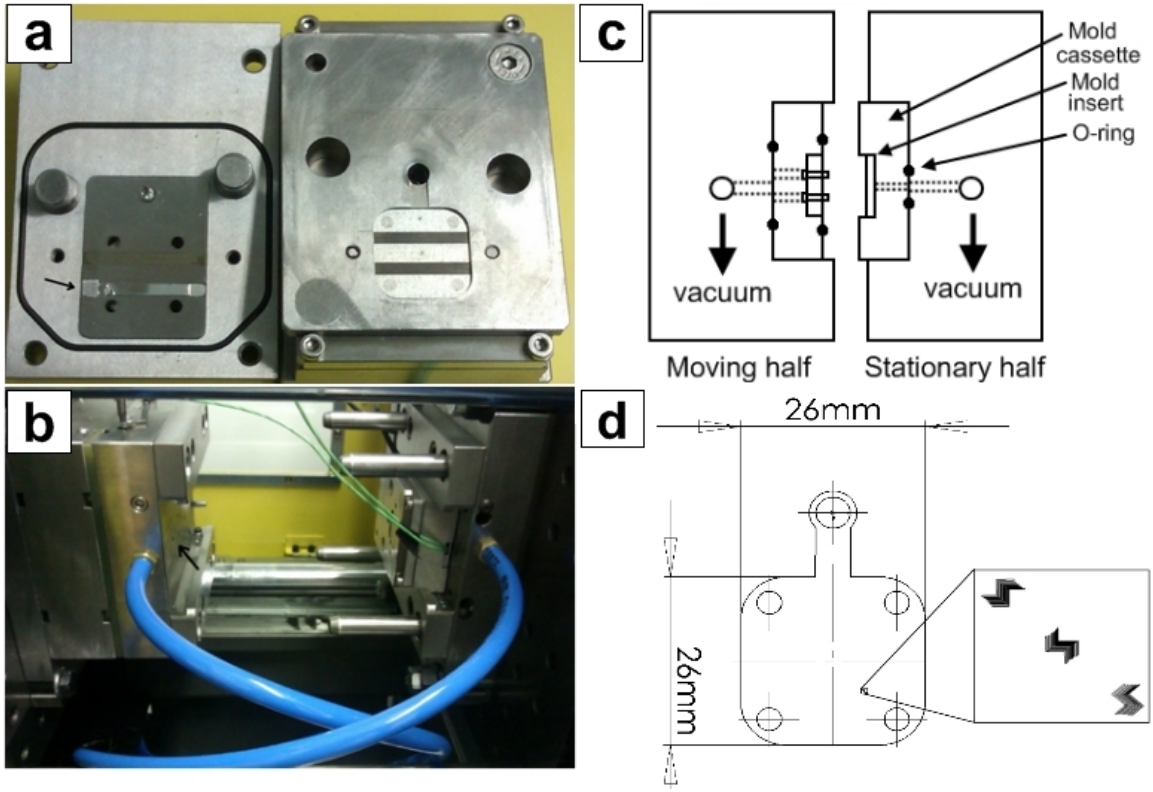

Fig. 1 (a) Cassette mold showing AAO mold template (arrow, left) and BMG mold strips (right); (b) cassette mold connected to vacuum pump; (c) illustration of mold cross-section; (d) sample shape (front view) and feature location for quantitative analysis.

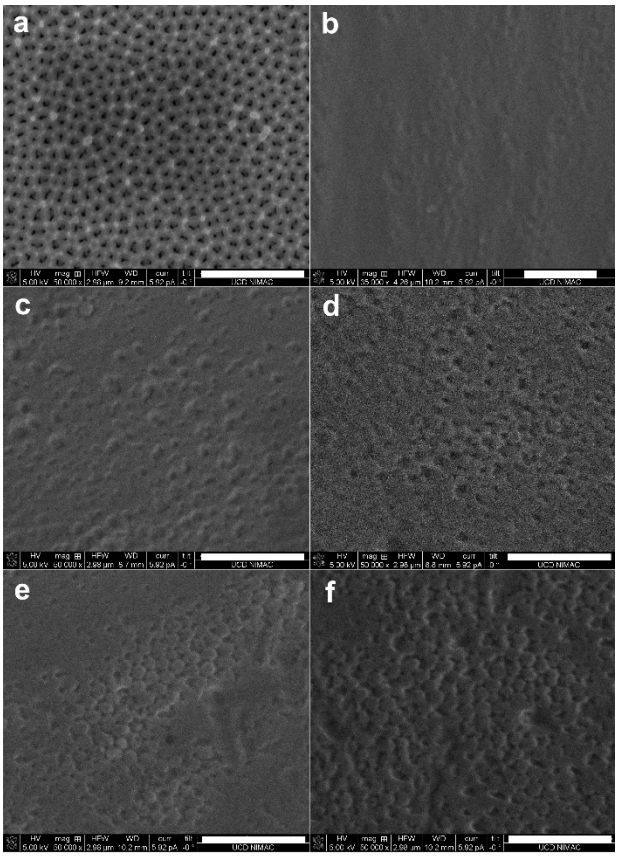

Fig. 2 SEM images of (a) AAO template, (b) COC samples under no vacuum, (c) COC sample under ~-33.25 kPa for 3 seconds, (d) COC sample under ~-65 kPa for 3 seconds, (e) COC sample under ~-33.25 kPa for 10 seconds; and (f) COC sample under ~-65 kPa for 10 seconds (scale bar: 1μm).

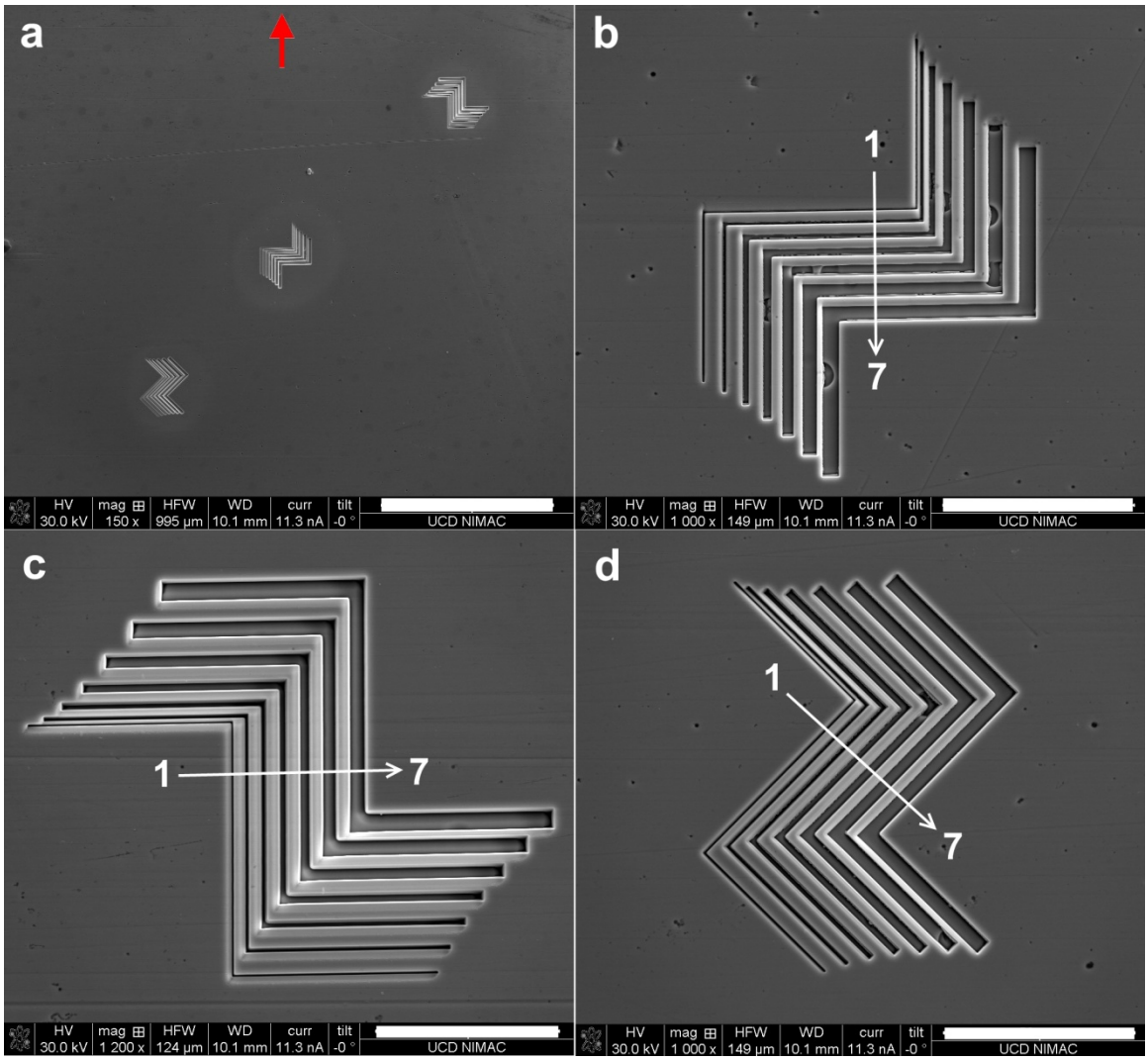

Fig. 3 SEM image of FIB features on BMG: (a) position of features (scale bar:300µm), (b) horizontal channels (scale bar: 50µm), (c) vertical channels (scale bar: 40µm), and (d) 45° channels (scale bar: 50µm). Red arrow represents direction of gate from the microfeatures.

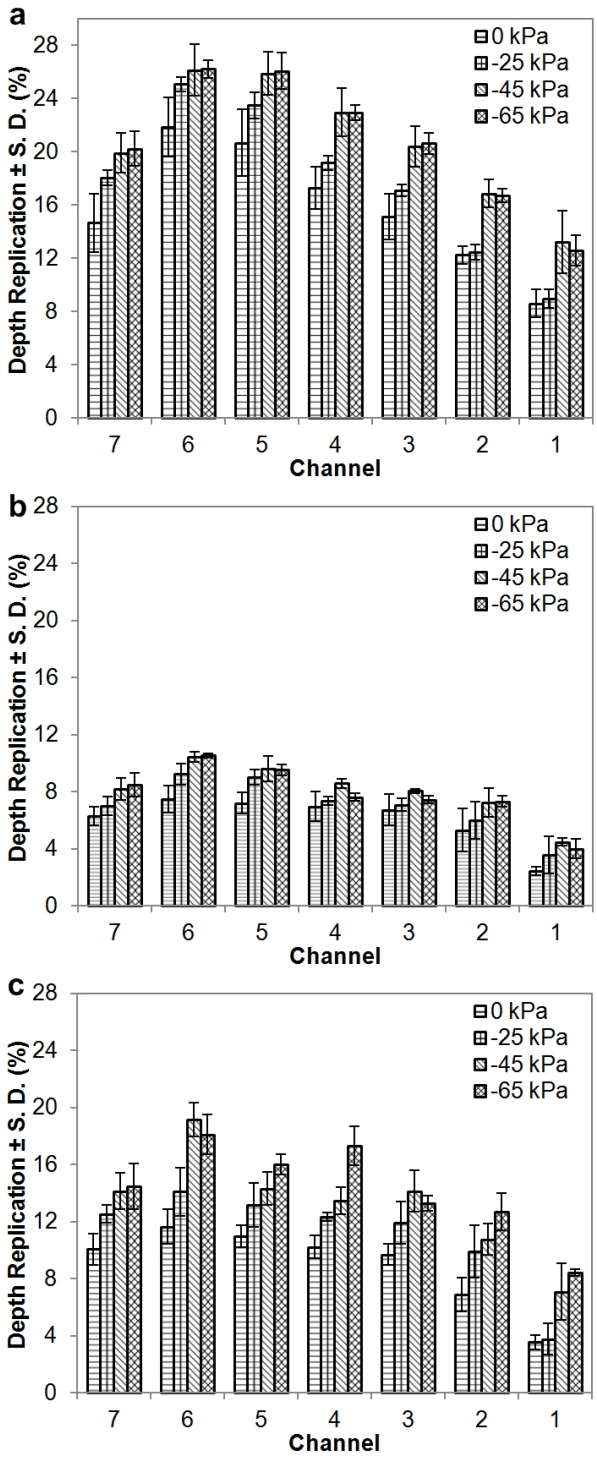

Fig. 4 Depth replication (%) as a function of maximum vacuum gauge pressure applied for (a) horizontal channels, (b) vertical channels, (c) 45° channels, at constant vacuum time 2s for channels 1-7 (n=3).

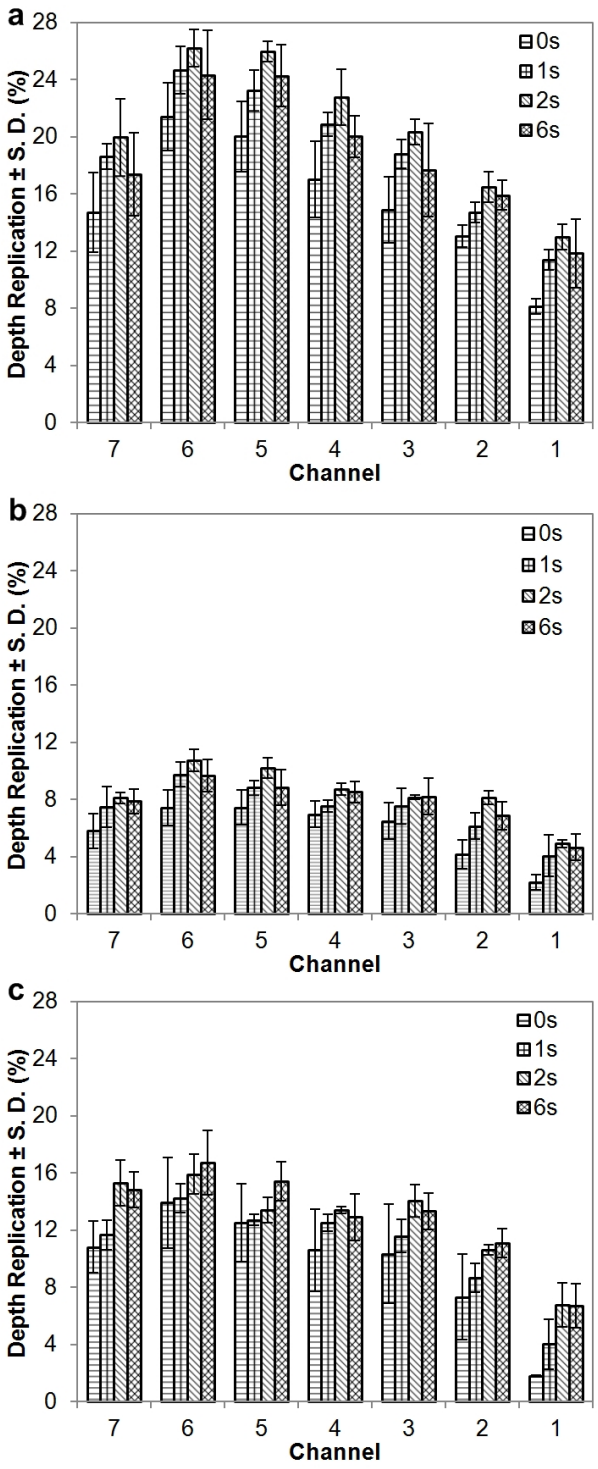

Fig. 5 Depth replication (%) as a function of vacuum time applied for (a) horizontal channels, (b) vertical channels, (c) 45° channels, at constant vacuum gauge pressure of ~45kPa for channels 1-7 (n=3).

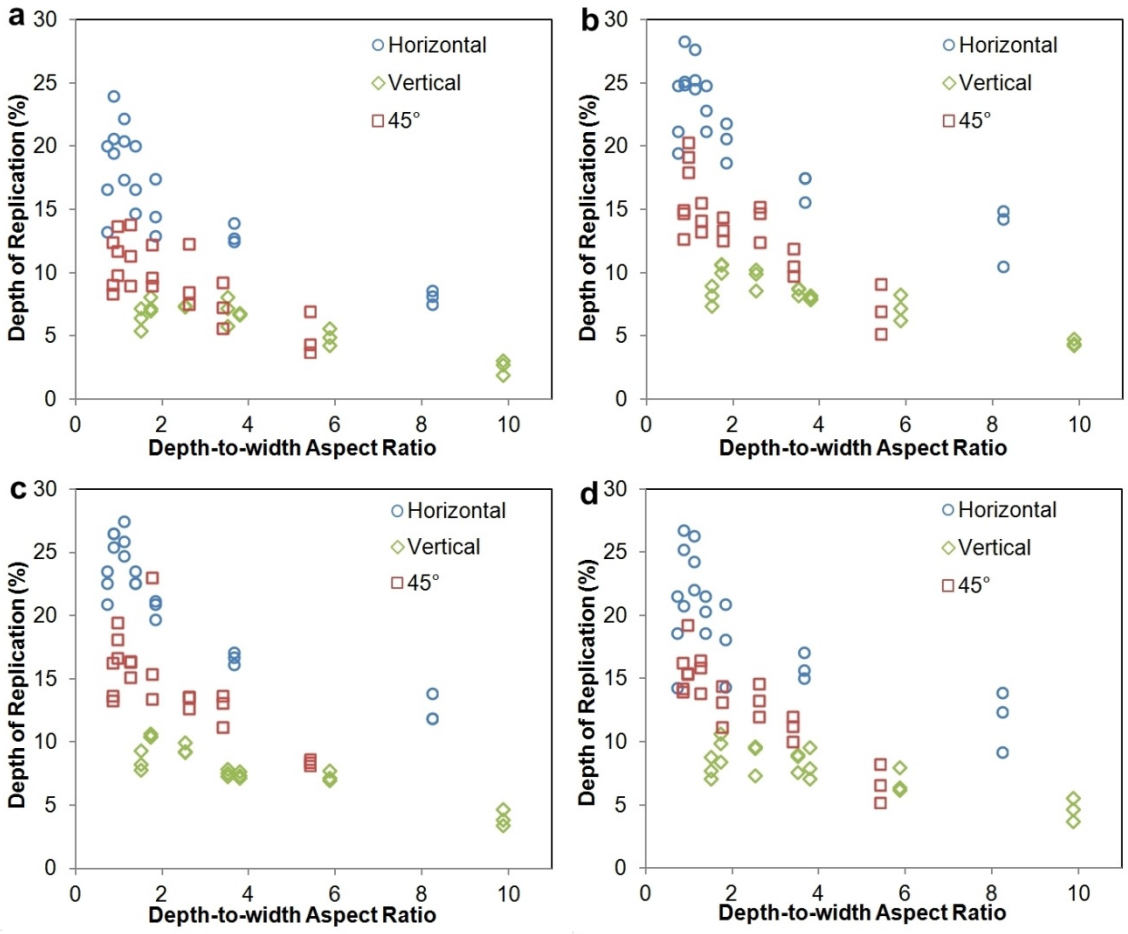

Fig. 6 Effect of different channel directions on depth of replication at (a) control condition (no vacuum applied), (b) maximum vacuum gauge pressure of ~-45 kPa at 2s vacuum time; (c) maximum vacuum gauge pressure ~-65kPa at 2s vacuum time; and (d) vacuum gauge pressure of vacuum time of ~-45 kPa at 2s vacuum time. Note: comparison of (b) and (c) for different vacuum gauge pressure and comparison of (b) and (d) for different vacuum time.

Table 1. Processing conditions for polymer samples.

Processing condition	COC 8007X10	PMMA VS-UVT
Hopper (°C)	40	40
Zone 1 (°C)	200	200
Zone 2 (°C)	208	207
Zone 3 (°C)	215	215
Nozzle (°C)	220	220
Injection velocity (mm/s)	150	150
Shot size (mm)	19	18
Holding pressure (MPa)	40	80
Holding Time (s)	1	1
Cooling time (s)	15	20
Mold temperature (°C)	70	60

Table 2. Calculated depth-to-width/ aspect ratio (A.R.) of the trenches in each channel direction.

	Horizontal		Vertical		45 degree	
Average Depth ± S.D. (μm) [a]	2.412±0.009		4.600±0.141		2.825±0.213	
Channel number	Average Width ± S.D. (μm)	A.R.	Average Width ± S.D. (μm)	A.R.	Average Width ± S.D. (μm)	A.R.
1 [b]	0.292±0.002	8.22	0.466 ± 0.046	9.86	0.523 ± 0.055	5.40
2	0.657±0.065	3.65	0.784 ± 0.024	5.86	0.835 ± 0.016	3.38
3	1.313±0.002	1.83	1.216 ± 0.081	3.78	1.083 ± 0.052	2.61
4	1.751±0.054	1.37	1.311 ± 0.063	3.51	1.605 ± 0.053	1.76
5	2.140±0.017	1.12	1.824 ± 0.061	2.52	2.269 ± 0.055	1.25
6	2.724±0.007	0.88	2.655 ± 0.070	1.73	2.926 ± 0.064	0.97
7	3.356±0.030	0.72	3.060 ± 0.070	1.50	3.378 ± 0.024	0.84

[a]Average depth is obtained from optical profilometer measurements (apart from channel 1).

[b]FIB results in same depth in each trenches within the same feature, confirmed by SEM.